

**Zeitschrift:** Helvetica Physica Acta  
**Band:** 34 (1961)  
**Heft:** VIII

**Artikel:** Absolute precision determination of several resonance and threshold energies and the  $\alpha$ -particle energy of  $\text{Po}^{210}$   
**Autor:** Rytz, A. / Staub, H.H. / Winkler, H.  
**DOI:** <https://doi.org/10.5169/seals-113205>

### **Nutzungsbedingungen**

Die ETH-Bibliothek ist die Anbieterin der digitalisierten Zeitschriften auf E-Periodica. Sie besitzt keine Urheberrechte an den Zeitschriften und ist nicht verantwortlich für deren Inhalte. Die Rechte liegen in der Regel bei den Herausgebern beziehungsweise den externen Rechteinhabern. Das Veröffentlichen von Bildern in Print- und Online-Publikationen sowie auf Social Media-Kanälen oder Webseiten ist nur mit vorheriger Genehmigung der Rechteinhaber erlaubt. [Mehr erfahren](#)

### **Conditions d'utilisation**

L'ETH Library est le fournisseur des revues numérisées. Elle ne détient aucun droit d'auteur sur les revues et n'est pas responsable de leur contenu. En règle générale, les droits sont détenus par les éditeurs ou les détenteurs de droits externes. La reproduction d'images dans des publications imprimées ou en ligne ainsi que sur des canaux de médias sociaux ou des sites web n'est autorisée qu'avec l'accord préalable des détenteurs des droits. [En savoir plus](#)

### **Terms of use**

The ETH Library is the provider of the digitised journals. It does not own any copyrights to the journals and is not responsible for their content. The rights usually lie with the publishers or the external rights holders. Publishing images in print and online publications, as well as on social media channels or websites, is only permitted with the prior consent of the rights holders. [Find out more](#)

**Download PDF:** 07.08.2025

**ETH-Bibliothek Zürich, E-Periodica, <https://www.e-periodica.ch>**

# Absolute precision determination of several resonance and threshold energies and the $\alpha$ -particle energy of $\text{Po}^{210}$

## PART I

by A. Rytz, H. H. Staub, and H. Winkler

Physik-Institut der Universität Zürich

(16. X. 1961)

*Zusammenfassung.* Es wurden Präzisionsmessungen der Energie der  $\text{T}(p, n)$ - und  $\text{Li}^7(p, n)$ -Schwelle sowie der  $\text{Po}^{210}$   $\alpha$ -Teilchen ausgeführt. Das gegenüber früheren Messungen weitgehend verbesserte magnetische  $180^\circ$ -Spektrometer hatte 0,04 bzw. 0,08 bzw. 0,15 mm weite Spaltblenden bei einem Bahndurchmesser von 1 m. Das Magnetfeld wurde mit Tonband-Folien homogen gemacht und Punkt für Punkt durch magnetische Kernresonanz ausgemessen. Eine weitere Kernresonanz-Sonde besorgte die Stabilisierung des Feldes auf besser als  $\pm 5 \cdot 10^{-6}$ . Der Van-de-Graaff-Beschleuniger wurde vom ca. 0,4 mm weiten Mittelspalt her stabilisiert. Die an dicken Targets gemessenen Schwellenwerte betragen  $(1019,35 \pm 0,20)$  keV für Tritium und  $(1880,48 \pm 0,25)$  keV für Lithium. Die  $\text{Po}^{210}$   $\alpha$ -Energie ergibt sich zu  $(5304,93 \pm 0,60)$  keV.

## Introduction

Precise determinations of a few calibration energies for nuclear spectrometers are needed in reaction energy measurements which in turn play an important role in nuclidic mass calculations<sup>1)</sup>.  $\text{Li}^7(p, n)\text{Be}^7$  threshold energy and  $\text{Po}^{210}$   $\alpha$ -particles are the most commonly used calibration standards. For  $\text{Li}^7(p, n)$  the threshold is now thought to be known rather accurately, whereas the  $\text{Po}^{210}$   $\alpha$ -energy is still under discussion. This uncertainty is mainly due to the specific behaviour of this element. Both these standards have repeatedly been measured during the past ten years by different methods (see table at the end). Direct comparison of the two calibration energies have, to our knowledge, been made in two cases only<sup>2) 3)</sup>, both of which are not beyond objection because of the quality of the sources used.

We have remeasured the energy of  $\text{Li}^7(p, n)$  threshold and of  $\text{Po}^{210}$   $\alpha$ -particles with a greatly improved absolute magnetic spectrometer. We believe this apparatus to be considerably less susceptible to unaccountable systematic errors than the one used by BUMILLER, STAUB and

WEAVER<sup>4</sup>) who initiated this technique in 1954. In addition, we have measured the lower-lying ( $p, n$ ) threshold of the  $T(p, n)He^3$  reaction. Part II<sup>5</sup>) is dealing with the  $Al^{27}(p, \gamma)Si^{28}$  resonance at 992 keV and the  $F^{19}(p, \alpha\gamma)O^{16}$  resonance at 872 keV. The  $F^{19}(p, n)Ne^{19}$  threshold measurement has been described separately<sup>6</sup>).

Monoenergetic  $\alpha$ -particles are most conveniently obtained, together with a reasonable half-life and without any other radiations present, from  $Po^{210}$ . However, these important advantages are greatly reduced by other well known and rather disturbing properties. It thus seems quite difficult to prepare thin, clean sources. The cleaner the source, the more it activates its neighbourhood by projection of active material under vacuum. Moreover, diffusion into the carrier material reduces the time during which  $Po^{210}$  sources can be used successfully. Some workers consider this time to be short, compared to 24 hours, others did not find any disturbing effect during several days. Nevertheless, it might be preferable to use a  $(Bi^{212} + Po^{212})$  source as energy standard<sup>7</sup>) despite its shorter life.

Although our experiment includes both  $Po^{210}$   $\alpha$ -particles and  $Li^7(p, n)$  threshold, we consider the values obtained as independent absolute measurements even though some of the contributing errors are correlated.

### General Method

The momentum of protons (originating from our 5.5 MeV Van de Graaff generator) and of natural  $\alpha$ -particles is measured by  $180^\circ$  deflection in a homogeneous magnetic field. The radius of curvature is determined by the distance between the entrance slit at  $0^\circ$  and the exit slit at  $180^\circ$  both of which are inside the homogeneous part of the field. Because of the focussing of particles with equal momentum after  $180^\circ$  deflection, the trajectory of the particles between these two narrow slits is somewhat arbitrary. All that is needed is a confinement of possible orbits by a diaphragm of relatively wide aperture. The field is measured by nuclear magnetic resonance (nmr) and the particle momentum is obtained by measurement of a length (distance between the slits,  $D_0$ , in cm) and a frequency,  $\nu_0$ , in cps.

The energy of the incident protons, expressed in the absolute eV scale, is given by (see, e. g. <sup>4</sup>)

$$V = \frac{\pi^2}{2\gamma_p} \frac{\nu_c}{\nu_k} D_0^2 \nu_0^2 (1 - \delta) \cdot 10^{-8} \text{ Volts ,}$$

where  $\gamma_p$  is the gyromagnetic ratio of the proton,  $\nu_c/\nu_k$  is the ratio of the cyclotron-frequency of the proton to its nmr frequency in the same field,  $\delta = eV/2M_0c^2$  is the first-order relativistic correction of the momentum-energy relation, and  $M_0$  is the proton rest mass.

The constants used in calculating absolute values of  $\alpha$ -particle kinetic energy are, besides  $\gamma_p$ , the Faraday number  $F$  and the atomic mass of  $\alpha$ -particles,  $M_\alpha$ . The energy amounts to

$$E = \frac{\pi^2}{\gamma_p^2} \frac{2F}{M_\alpha} D_0^2 v_0^2 (1 - \delta') \cdot 10^{-5} \text{ keV}.$$

Here again,

$$\delta' = \frac{1}{2} \frac{F}{M_\alpha} \frac{10^{17} E}{c^2}$$

is the first order relativistic correction. For the constants the following values have been used:

$$\left. \begin{aligned} \gamma_p &= 26751.3 \pm 0.2 \text{ s}^{-1} \text{ G}^{-1}, \\ v_k/v_c &= 2.79268 \pm 0.00006, \\ F &= 9649.12 \pm 0.11 \text{ emU/Mole}, \\ M_\alpha &= 4001506.5 \pm 0.4 \mu \text{ MU}, \end{aligned} \right\} (\text{C}^{12} \text{ scale}).$$

### Experimental Set-up

The magnet used in these experiments has been designed specially for absolute measurements and has been described by WINKLER and ZYCH<sup>8)</sup>. The pole pieces of 140 mm width covered an angular length of 210°. The gap was 24 mm wide. The central orbit for particles which passed through the magnet had a radius of 500 mm. Nuclear magnetic resonance together with a current-stabilizing circuit provided a field stability of better than  $\pm 5$  parts in  $10^6$ . The frequency of the nmr probe determined the magnetic field strength through the intermediary of the stabilizing circuit. The same frequency was taken as abscissa in plotting yield curves. The probe was located at 106° behind the entrance slit and at a radial distance of 525 mm. Frequencies could be determined to better than  $\pm 20$  cps by means of a frequency decade 'Schomandl ND 5'. The quartz oscillator of the decade could be calibrated with standard frequencies to better than  $\pm 5$  parts in  $10^7$ .

The field in the whole region between the pole faces has been mapped carefully, and shims have been prepared in order to obtain a very homogeneous field. Magnetic recording tape has proved very convenient for this purpose<sup>8)</sup>. Nowhere in the region considered between the two slits did the field strength differ from the mean value by more than 1.5 parts in  $10^4$ . This homogeneous region had a radial dimension 25 times as wide as the proton beam (twice that of the  $\alpha$ -particle beam). We prepared

three different sets of shims to be used with the three different field settings.

The field was measured point by point by means of a second 8 mm long cylindrical nmr probe of 3 mm diameter, filled with 1/30 *n* aqueous solution of  $\text{MnSO}_4$ . The cylinder axis was tangent to the particle orbit. Two ball bearings in the geometrical central axis of the magnet allowed the probe to be moved smoothly along the circular orbit, and the radial position could be adjusted by means of a spindle. The probe could thus be placed at any point in the central plane of the gap with a precision of  $\pm 0.5$  mm. A complete set of measurements consisted of 45 points on the central orbit and, in some cases, of two additional series of 45 points each on a circle 5 mm inside and outside the central path. The effective field  $B_0$  was obtained from the value  $B$  measured by the stabilizing probe with the first order Hartree correction<sup>9</sup>):

$$B_0 = B + \frac{1}{2} \int_{0^\circ}^{180^\circ} \Delta B(\vartheta) \sin \vartheta d\vartheta.$$

$\Delta B$  is the field on the central orbit at an angle  $\vartheta$  minus the field given by the stabilizing probe. All Hartree corrections were less than  $5 \times 10^{-5}$  of  $B_0$  and were obtained as an average of two measurements, before and after the runs. The assessed errors of the Hartree corrections, as indicated under 3) in Table 2, were always greater than one half of the difference between the two corresponding measurements. The corrections were found not to vary with the value of the field over a range considerably greater than actually used. The vacuum chamber could be mounted without switching off the nmr stabilization system.

A microwave wave-guide, bent to the correct radius, was used for the vacuum chamber. Besides the mercury diffusion pump of the Van de Graaff accelerator acting on the entrance side, there was an additional Hg pump evacuating the target chamber with a speed of 600 l/sec. It was equipped with a liquid air trap. Nowhere in the chamber did the pressure exceed  $10^{-4}$  mm Hg, whereas in the target chamber it was never above  $2 \times 10^{-6}$  mm Hg. The presence of the vacuum chamber did not give any detectable change in field strength (more than 5 parts in  $10^6$ ), due to the finite susceptibility of its material.

The slits at  $0^\circ$  and  $180^\circ$  were mounted on a single piece of molybdenum rod of 10 mm diameter which could be introduced easily into the vacuum chamber. When the slits were in their working position on a diameter of the central orbit, the full cross section of the molybdenum rod was located outside the central axis of the magnet by about 2 mm. This axis was defined by a 0.2 mm steel wire passing through the centre holes of the crank shaped pivot carrying the field measuring device. With the projec-

tion of the centre mark on the rod surface passing through the steel wire, the two momentum defining slits were situated on the circle described by the nmr probe during the preceding field measurement within  $\pm 0.5$  mm. The diaphragms at  $0^\circ$  and  $180^\circ$  each consisted of two firmly stretched tantalum-wires of 0.2 mm diameter as recommended by BASTIN and WALEN<sup>10</sup>). This construction minimizes scattering effects, has smooth defining surfaces and is easily cleaned. The distance between the centres of the slits was measured before and after the experiment by the Swiss National Bureau of Standards in Berne using a comparator and a standard meter bar\*). In addition, we measured the slit distance by the method used in all our earlier absolute energy determinations. The same result was obtained, within the errors, but less accurate. Slit widths have been determined under a measuring microscope. In order to keep away from the diaphragm as many dispensible protons as possible, a movable gold sheet with a 0.2 mm slit was placed in front of the entrance slit. The proton current hitting the entrance slit was thus kept below  $1 \mu\text{Amp}$ . In the case of Po  $\alpha$ -particles the gold sheet was not used. A source carrier could be introduced instead, which held the source at a distance of about 8 mm from the slit, and which could be adjusted under vacuum.

At  $\vartheta = 90 \pm 1^\circ$  a third slit defined the aperture of the beam. When measuring proton energies, the two insulated halves of the middle slit were used, in a well known manner, for the stabilization of the Van de Graaff voltage by means of a grid-controlled corona discharge. Because the proton beam was well collimated, slit widths of 0.2 to 0.4 mm could be used. However, in the case of Po  $\alpha$ -particles, the middle slit had to be opened to 6 mm in order to get sufficient intensity.

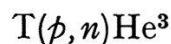
The radial position of the middle slit could be determined with the aid of the centre wire to  $\pm 0.5$  mm. Three points of the mean particle orbit thus coincided within  $\pm 0.7$  mm with the circle described by the field measuring probe. Further it is certain that the circle passing through entrance and exit slits with a diameter equal to their distance passes within 0.7 mm through the centre of the middle slit. Together with the width of the latter this 0.7 mm defines the maximum angle  $\beta$  between an actual particle orbit and the corresponding tangent at the above mentioned circle. If  $\beta$  is small the image of the entrance slit in the plane of the exit slit is shifted inwards by  $D_0 \beta^2/4$ , provided that the energy remains unaltered. For protons this shift did not exceed 3 microns and thus was neglected. In the case of  $\alpha$ -particles a 6 mm wide aperture was used. A special treatment of the properties of the spectrometer for this arrangement will be given later.

---

\*) We wish to thank Dr. W. LOTMAR from the «Eidg. Amt für Mass und Gewicht» (Dir. Prof. H. KÖNIG) for kindly measuring the slit distance.



### Discussion of measurements



Out of a total current ( $H_1^+ + H_2^+$ ) of approximately 5  $\mu$  Amps about  $3 \times 10^{-2}$   $\mu$  Amps could be directed to the target. This current was measured by a precision integrating circuit. The target consisted of a tritiated zirconium disc obtained from Radiochemical Centre, Amersham, England. The tritium concentration of these targets is known<sup>11)</sup> to be critically dependent on the depth below the surface. Therefore very high resolution was used and measurements were confined to an energy region as close to the threshold as possible. The triangular energy distribution behind the exit slit had a half-width of 80 eV.

For a thick and homogeneous target, and for a detector counting all neutrons with equal efficiency, the  $2/3$  power of the neutron yield depends linearly on proton energy, provided measurements are made a few keV only from threshold and no narrow energy level of the compound nucleus exists near threshold (see, e. g.,<sup>12)13)</sup>). Neutron yields to the  $2/3$  power obtained in three subsequent runs up to 2 keV above threshold could be fitted well to a straight line with a correlation coefficient of 0.95 (Fig. 1). We therefore conclude that, owing to the small energy interval, an inhomogeneous tritium distribution in the target could not have influenced the measurements. A best fit straight line through the points obtained (neutron yield to the first power) gave a correlation coefficient of 0.73 and a threshold energy 150 eV higher.

Neutrons were detected by an enriched  $B^{10}$  plastic scintillator (Nuclear Enterprises Ltd.), 1 mm thick and 50 mm diameter (5%  $B^{10}$  by weight). The axis of this disc shaped detector coincided with the proton direction at the target. The detector was fixed at 20 mm behind the target. A 10 mm thick paraffin disc of 80 mm diameter served as a moderator and was placed immediately in front of the scintillator disc. A 12 mm thick plexiglas light-guide behind the scintillator was an additional moderator and neutron-reflector. Neutrons emitted from the target within an angle of  $45^\circ$  with respect to the proton direction could reach the counter. Since the maximum proton energy was 2 keV above threshold, the emission angles of neutrons varied between  $0^\circ$  and  $18^\circ$ . Furthermore, the mean neutron energy ( $E_n = 64$  keV at threshold) did not vary much in this range. Consequently, the counting efficiency was nearly constant.

In order to prevent the formation of carbon layers on the target, it was heated to about  $100^\circ\text{C}$ . In three subsequent threshold runs no shift of the threshold energy towards higher values could be observed. Therefore no distinction is made between these three runs. The data pertaining to these runs are shown in Table 1. Table 2 gives the components of the

error in the final result. It should be kept in mind that no contribution to the error in the threshold energy has been assessed for target condition (e. g. for a well-defined thin surface layer free of tritium). Several targets of equivalent type have been carefully investigated by BONDELID *et al.*<sup>13)</sup>. No threshold shift due to target quality has been observed. Nevertheless we plan to remeasure the threshold energy with a T<sub>2</sub>O ice target. This is particularly desirable, if the result is to be used for calculating the neutron hydrogen mass difference rather than for energy calibration.

Table 1  
Data of the threshold measurements

Target	converted by water vapour into LiOH	same as in 1 <sup>st</sup> col.	LiF	tritiated zir- conium
Temperature of molybdenum rod (°C)	25.2	26.4	27.2	19.4
Slit distance (mm) . . . . .	1 000.071	1 000.079	1 000.084	1 000.101
Slit width (entrance and exit) (mm)	0.08	0.08	0.08	0.04
$\nu_{ex}$ (kcps) . . . . .	16 880.30	16 880.05	16 879.90	12 424.2
Hartree correction (kcps) . . . . .	- 0.32	- 0.32	- 0.32	+ 0.44
Threshold energy (keV) . . . . .	1 880.51	1 880.48	1 880.46	1 019.35

Table 2  
Absolute standard errors, expressed in frequency (kcps)

Source of error	Li <sup>7</sup> ( <i>p</i> , <i>n</i> )Be <sup>7</sup>	T( <i>p</i> , <i>n</i> )He <sup>3</sup>
1) $\nu_{ex}$ . . . . .	± 0.2	± 0.7
2) Asymmetrical energy distribution of protons behind the exit slit as a result of asymmetrical stabilization of the Van de Graaff voltage . . . . .	± 0.7	± 0.3
3) Hartree correction, including reading error of nmr signal on oscilloscope . . . . .	± 0.5	± 0.5
4) Measurement and stability of frequency (field) during runs . . . . .	± 0.05	± 0.05
5) Distance between slits, including uncertainty of temperature of the molybdenum rod . . . . .	± 0.4	± 0.3
6) Constants used for calculation of threshold	± 0.3	± 0.2
Combined error . . . . .	± (1.03) <sup>1/2</sup> kcps	± (0.96) <sup>1/2</sup> kcps
Absolute energy value . . . . .	± 250 eV	± 200 eV



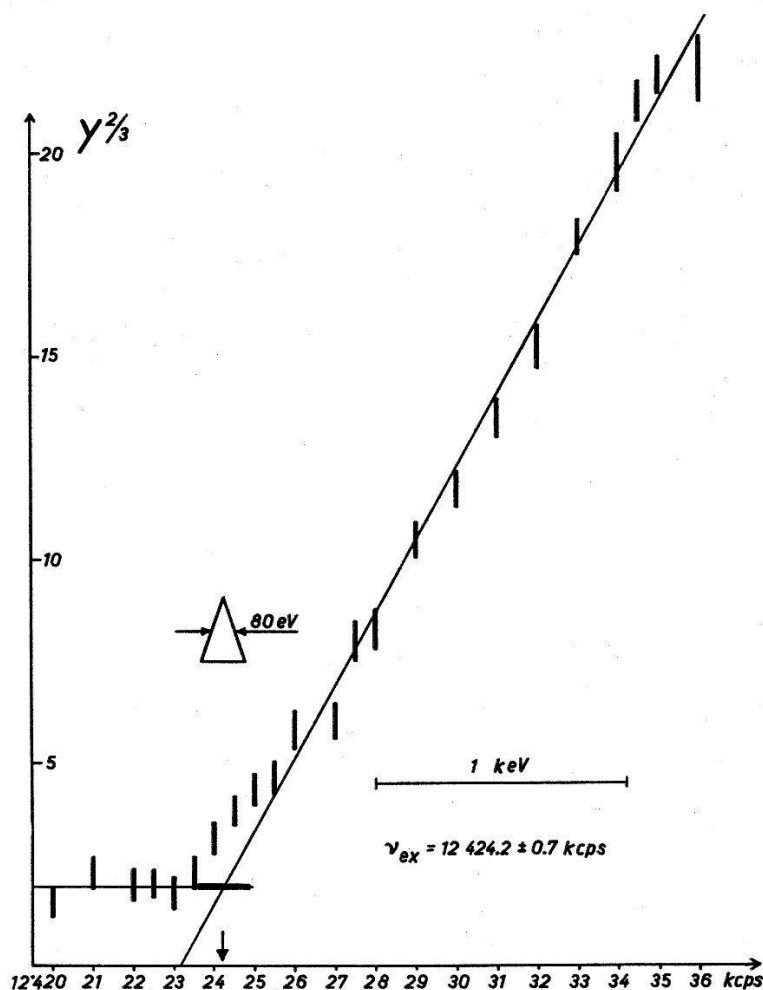
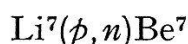


Fig. 1

(Neutron yield) $^{2/3}$  from  $T(p, n)$  reaction versus spectrometer field strength (expressed in kcps). The straight line was calculated by least squares from all points above 12424.5 kcps. Counting and frequency errors are shown to scale. The triangle represents the probable energy distribution of the protons at the target.



A mean target current of about  $4 \times 10^{-2} \mu\text{Amps}$  was used and measured in much the same way as in  $T(p, n)$  measurements. Three different runs have been completed, with targets obtained from an evaporated layer of lithium metal, converted into LiOH with water vapour (run I and II) and of LiF (run III) (see Table 1). No additional cold traps were used nor were the targets heated. Instead, a 6 cm long plate condenser was placed between the exit slit and the target. An a. c. voltage of 2 kV, 50 cps, applied to the condenser extended the region on the target hit by the proton beam from  $0.2 \times 8 \text{ mm}^2$  to  $3 \times 8 \text{ mm}^2$ . The considerably smaller proton number per unit target surface decreased the danger of carbon layers being formed. In addition electrostatic charging of the target sur-

face became much less probable. The energy range used was covered twice during each run. No systematic shift of threshold energy by building up of carbon layers has been observed.

The same arrangement of neutron detection was used as described in the  $T(p, n)$  experiment, but with a scintillator of 75 mm diameter. The maximum accepted neutron emission angle would have been  $55^\circ$ . However at the highest energy used (2 keV above threshold) the maximum emission angle was only  $13^\circ$ . Also, in this case, the mean neutron energy did not vary much in the small energy interval chosen.

Figure 2 shows, as an example, the results ( $2/3$  power) of the first run. Disregarding the cusp due to the finite resolution of the spectrometer, the measured neutron-yields fit well into a straight line with the excellent correlation coefficient of 0.992. All points of this run have been considered according to their weights as given by the statistical error of each measurement. We may conclude that the detector had a constant efficiency in the small energy interval considered. If we plot the neutron yield to the first power (Fig. 3), the result deviates very definitely from a straight line. The same data as in Figure 2 have been used and weights have been considered similarly. This straight line yields a correlation coefficient of 0.91 and would lead to a threshold value 220 eV higher. From Figure 3 it is evident that the result of the direct extrapolation depends considerably on the energy interval used and on the extrapolation procedure. All the early results which were obtained by direct linear extrapolation should therefore be considered with care \*).

The three threshold values as obtained from the three different runs coincide within 50 eV. Table 2 shows the components of the errors in the final results.

### *Polonium $\alpha$ -particles*

$Po^{210}$  is still used extensively as an energy standard, despite its well-known detrimental properties. It therefore seemed desirable to make a new absolute measurement of this energy value with our spectrometer. Several careful absolute determinations of this energy have been published during the last decade<sup>7) 14) 15)</sup>.

---

\*) *Note added in proof:* Recently, BECKNER *et al.*<sup>21)</sup> published measurements of neutron threshold energies in which a linear extrapolation of yield curves to the first power was used and the error introduced by the linear law is compensated by effects of finite resolution and target thickness. Although the errors due to this procedure are probably small, it seems to us quite objectionable since calculated  $2/3$  power yield curves with finite but high resolution show only minute deviations from linearity, well within the statistical errors of those measured points used for the extrapolation (cf. Figure 2). At 16881.5 kcps the calculated deviation from the straight  $Y^{2/3}$  line, due to the finite resolution, is less than 2%.

Thin sources have a limited intensity. Therefore all the slits had to be wider than in the preceding experiments. We chose 6 mm for the middle slit and 0.15 mm for the other two. A solid state detector (silicon  $p$ - $n$ -junction) was placed 10 mm behind the exit slit. At the time the only detector available was a circular disc of 2 mm diameter.

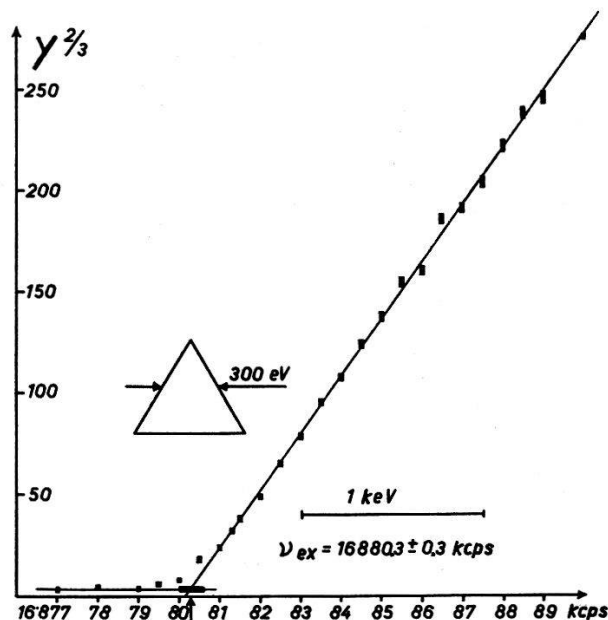


Fig. 2

(Neutron yield)<sup>2/3</sup> from  $\text{Li}^7(p, n)$  reaction versus spectrometer field strength (in kcps). The points shown (run I, LiOH, with counting and frequency errors to scale) fit well into the least squares adjusted straight line (correlation coefficient 0.992), as obtained from all the points above 16881.5 kcps. For the triangle, see Figure 1. The extrapolated threshold is indicated by an arrow.

The quality of every  $\text{Po}^{210}$   $\alpha$ -measurement depends to a high degree on the source properties. The most successful procedure<sup>7)</sup> seems to consist in deposition by volatilization in vacuum on a polished tantalum surface. Our source has been prepared by the 'Laboratoire de l'Aimant Permanent' at Orsay (France), where this technique has been developed by R. J. WALÉN as described in <sup>16)</sup>. The polonium had been deposited on only one narrow side ( $8 \times 0.3 \text{ mm}^2$ ) of a piece of tantalum  $10 \times 8 \times 0.3 \text{ mm}^3$ , which had been polished previously. The distribution of the activity of about  $50 \mu\text{c}$  may have been rather uneven. This was partly compensated by the fact that the slit width was only half of the source width. Moreover, the source could be shifted across the slit under vacuum. Before starting a run, the source was centered with respect to the slit by maximizing the counting rate with a field setting corresponding to the horizontal part of the line.

The source thickness was found to be of the order of 12 keV. This is considerably more than expected, but was probably due to impurities in the primary polonium as obtained from Radiochemical Centre, Amersham.

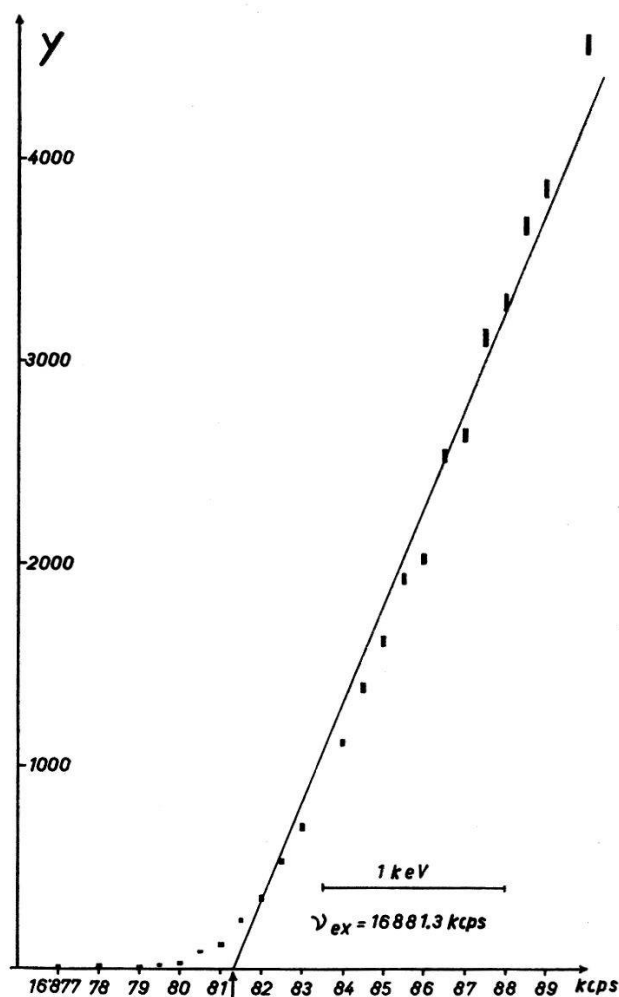


Fig. 3

Neutron yield from  $\text{Li}^7(p, n)$  reaction versus spectrometer field. Same data as in Figure 2. The fit into the least squares adjusted straight line, calculated from all points above 16881.0 kcps, is less good (correlation coefficient 0.91).

A high residual activity of the surroundings after taking off the source is a certain indication for a clean source. We therefore believe that the source was not covered by an important inactive absorbing layer. However, it must be emphasized that systematic errors arising from source properties are not considered in our error. The rather localized contamination of the spectrometer did not reach the detector region during the experiment. No increase of background  $\alpha$ -particles was present. A slight initial and constant contamination of the detector could be measured accurately.

Three spectra have been measured by observing the counting rate as a function of magnetic field strength, i. e. nmr frequency. Most of the points were chosen on the high energy edge of the line. This part of the spectrum of the third run, which was the most accurate one, is represented in Figure 4. The source age was 8 days by then.

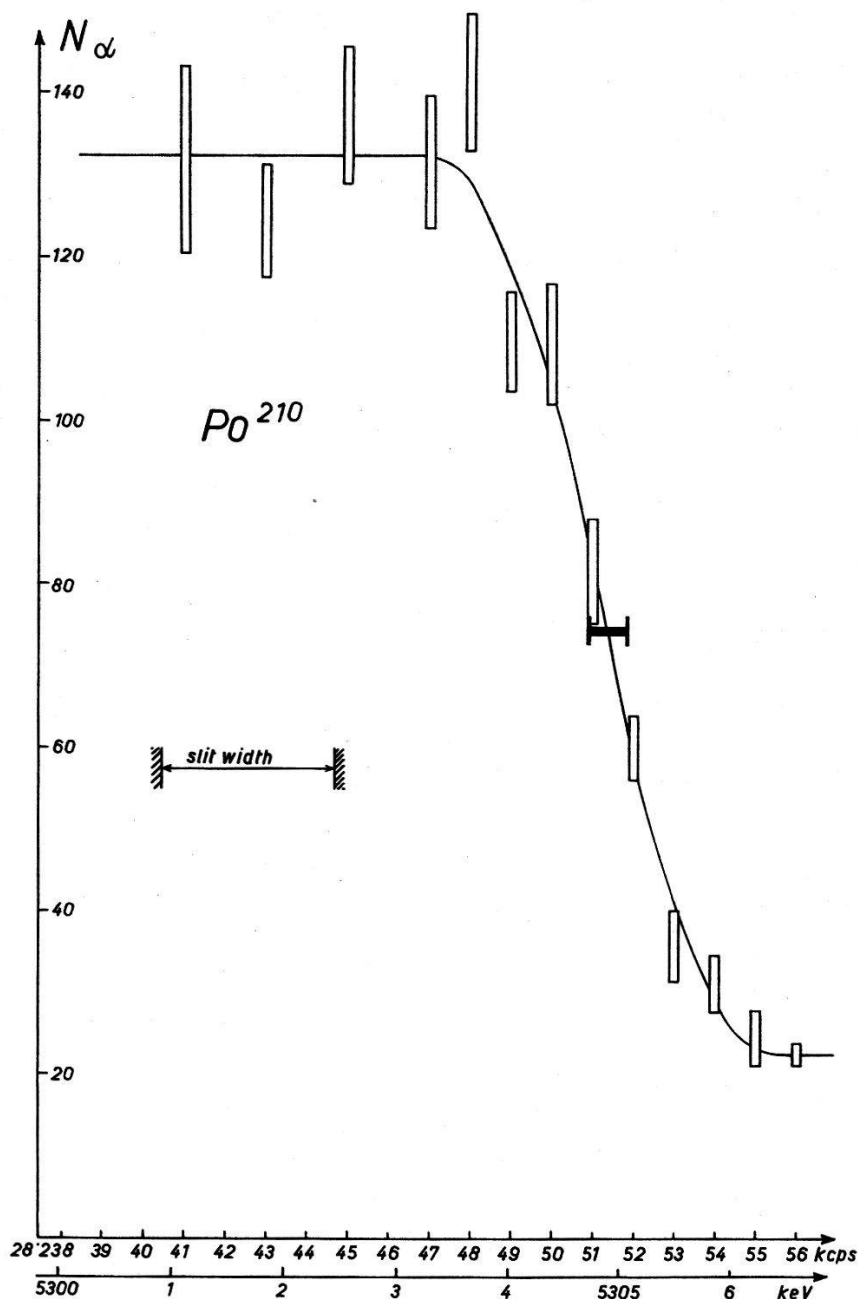


Fig. 4

$\text{Po}^{210}$   $\alpha$ -particles per 20 minutes versus spectrometer field (run III). The curve gives the theoretical line shape. Its position was adjusted by least squares. The experimentally obtained  $v_{ex}$  with its error is shown at the steepest point of the high energy edge. The line width at the base would correspond to a source thickness of 12 keV. Counting and frequency errors are shown to scale.

For the calculation of the theoretical line shape we follow the procedure outlined by COLLINS *et al.*<sup>14</sup>). Although in our measurements the distance  $D$  between the slits was kept constant, and a variable magnetic field was used, the problem is most easily discussed in terms of a constant field and a variable slit distance. The two pictures are exactly equivalent. The point at which we want to calculate the relative intensity is characterized by the coordinate  $x$ , i. e. the distance between this point and some arbitrary zero point. With  $x=0$  we mean the point hit by an  $\alpha$ -particle which has the greatest possible distance from the source. Increasing  $x$  corresponds to decreasing momentum. The relative intensity  $F(x)$ , for a monoenergetic source, at the point  $x$ , is given by:

$$\begin{aligned} F(x) &= A \arcsin \left( \frac{x}{\varrho} \right)^{1/2} && \text{for } 0 < x < \frac{a^2}{\varrho}, \\ F(x) &= B \arcsin \frac{a}{\varrho} && \text{for } \frac{a^2}{\varrho} < x < s, \\ F(x) &= B \left( \arcsin \frac{a}{\varrho} - \arcsin \left( \frac{x-s}{\varrho} \right)^{1/2} \right) && \text{for } s < x < s + \frac{a^2}{\varrho}, \end{aligned}$$

with  $a$ : half width of middle slit,  
 $\varrho$ : radius of particle orbit,  
 $s$ : width of entrance slit,  
 $A, B$ : constants.

A thick homogeneous source may be thought of as made of a great number of very thin layers. The depth below surface corresponds to a shift in the spectrum. Integration over the source thickness  $d$  results in a relative intensity  $F'(x)$  at  $x$ :

$$F'(x) = \int_0^d F(x - x') dx', \quad \text{where } \left. \begin{array}{l} x' < x \\ x' < d \end{array} \right\}.$$

By integrating over the exit slit of equal widths we get for the counting rate:

$$I(x) = \int_{x-s}^x F'(\xi) d\xi.$$

Now the coordinate  $x$  must be converted into frequency of the stabilizing nmr probe. This new variable is  $\nu_x = \bar{\nu} x/2\varrho$ , where  $\bar{\nu}$  is the frequency corresponding to the energy of the particles. The integration is most easily carried out graphically and gives the curve shown in Figure 4. The most probable position of this curve was found by least squares adjustment and yielded the experimentally defined frequency  $\nu_{ex}$  and its



standard deviation. The data and error contributions of the three runs are given in Table 3. From  $\nu_{ex}$ , after applying the Hartree correction, the energy was calculated in a straightforward manner. The three values obtained coincided within 740 eV but differed in precision slightly. By assigning relative weights of 1, 2, 5 respectively, the final result was calculated, retaining the error of the last spectrum. The three errors were, of course, highly correlated.

Table 3  
Data of the  $\text{Po}^{210}$ - $\alpha$ -energy measurements

No. of run	I	II	III
Total duration (h) . . . . .	8	4	12
Temperature of molybdenum rod ( $^{\circ}\text{C}$ )	27.0	25.0	25.0
Slit distance (mm) . . . . .	1 000.010	999.997	999.997
$\nu_{ex}$ (kcps) . . . . .	28 249.32	28 252.20	28 251.33
Hartree correction (kcps) . . . . .	+ 0.60	+ 0.07	+ 0.27
Absolute standard errors (kcps)			
1) $\nu_{ex}$ (see Table 2) . . . . .	$\pm 0.6$	$\pm 0.6$	$\pm 0.5$
2) Asymmetry of source position and activity distribution . . . . .	$\pm 1.3$	$\pm 1.2$	$\pm 1.1$
3) Hartree correction (see Table 2) . . . . .	$\pm 0.6$	$\pm 0.4$	$\pm 0.4$
4) Frequency measurement: (see Table 2) . . . . .	$\pm 0.12$	$\pm 0.12$	$\pm 0.12$
5) Slit distance (see Table 2) . . . . .	$\pm 0.7$	$\pm 0.7$	$\pm 0.7$
6) Constants used for calculation. .	$\pm 0.4$	$\pm 0.4$	$\pm 0.4$
Combined error (run III) . . . . .	$\pm (2.3)^{1/2}$ kcps		
Absolute energy value (run III) . . . . .	$\pm 600$ eV		

## Results

Table 4 shows our results together with the most important earlier determinations. The measurements of threshold energies made with an absolute electrostatic analyzer by BONDELID *et al.*<sup>12) 17)</sup> and by a time of flight method by SHOUPP *et al.*<sup>18)</sup> agree well with our values. Still better agreement, for  $\text{Li}^7(p, n)$ , is reached by plotting Bondelids neutron-yields to the power  $2/3$ . The extrapolation then gives 1881,1 keV.

Our  $\text{Po}^{210}$   $\alpha$ -energy value agrees perfectly with the Orsay result<sup>7)</sup> which was obtained in a permanent magnet, using photographic plates instead

of an exit slit and a smaller radius of curvature. The agreement with the result of COLLINS *et al.*<sup>14)</sup> is equally good. There, an apparatus rather similar to ours has been used. WHITE *et al.*<sup>15)</sup> obtained their value in a completely different way. It too agrees well with ours within the errors quoted. The reason of the discrepancies between various measurements of  $\text{Po}^{210}$   $\alpha$ -energy lies above all in the different techniques of source preparation. Early relative measurements, however carefully done, contribute to the confusion. Some workers would even prefer to know the energy from an 'actual average source'. We do not think that this procedure would improve the present state of affairs. There is little doubt that the sources of earlier measurements were less trustworthy than those of the later experiments. Since there are now four or five new precise measurements agreeing fairly well among each other, it seems reasonable trying to get rid of possible systematic errors by discarding most of the older experiments.

Table 4  
Results and comparison to earlier values (keV)

$\text{T}^3(p, n)\text{He}^3$ . . . .	BONDELID <i>et al.</i> <sup>13)</sup> . . . . .	1019.7 $\pm$ 0.5
	present work . . . . .	1019.35 $\pm$ 0.2
$\text{Li}^7(p, n)\text{Be}^7$ . . . .	SHOUPP <i>et al.</i> <sup>18)</sup> . . . . .	1881.2 $\pm$ 1.9
	BONDELID <i>et al.</i> <sup>17)</sup> . . . . .	1881.2 $\pm$ 0.9
	STAUB and WINKLER <sup>12)</sup> . . . .	1880.3 $\pm$ 0.5
	BECKNER <i>et al.</i> <sup>21)</sup> . . . . .	1880.5 $\pm$ 0.8 *)
	MARION <sup>22)</sup> (calculated mean) . .	1880.7 $\pm$ 0.4
	present work . . . . .	1880.48 $\pm$ 0.25
$\text{Po}^{210}\alpha$ -particles . .	COLLINS <i>et al.</i> <sup>14)</sup> . . . . .	5304.8 $\pm$ 2.9
	WHITE <i>et al.</i> <sup>15)</sup> . . . . .	5305.4 $\pm$ 1.0
	RYTZ <sup>7)</sup> . . . . .	5304.81 $\pm$ 0.62
	EVERLING <i>et al.</i> <sup>19)</sup> (calculated) .	5302.8 $\pm$ 1.0
	BECKNER <i>et al.</i> . . . . .	5302.5 $\pm$ 1.5 *)
	present work . . . . .	5304.93 $\pm$ 0.60
(corresponding $H \cdot q$ )		331 778 $\pm$ 19 G $\cdot$ cm)

Since many nuclear reaction measurements have been made relative to the  $\text{Po}^{210}$   $\alpha$ -energy, EVERLING *et al.*<sup>19)</sup> introduced this energy as a variable for nuclidic mass calculations. By a least squares adjustment he then found an energy value which nearly coincided with some average result which WAPSTRA<sup>20)</sup> in 1960 calculated from direct measurements ranging between 1932 and 1958, including relative measurements based on BRIGGS's

\*) Note added in proof: Using the more recent value for  $\gamma_p^{23}$  (as we did in the present work), one would get 1880.57 and 5302.9 respectively, in fair agreement with our results.

Po<sup>214</sup> value (1936). However, EVERLING's value (see Table 4) conflicts seriously with recent absolute determinations. Clearly, corrections should be made, as WAPSTRA points out himself, for target thickness (and source properties), but this cannot be done without arbitrariness. We believe that, because of the difficulties encountered in estimating these errors, the result of the calculations proposed by EVERLING *et al.* is always less reliable than a carefully made direct measurement.

In an informal progress report to the IUPAP commission on nuclidic masses (letter of 5<sup>th</sup> Sept. 1961), J. W. M. DU MOND stated provisional, new values of some fundamental constants among them the Faraday and the gyromagnetic ratio of the proton in water. They would lower our Po<sup>210</sup> result by 200 eV.

### Acknowledgments

We are greatly indebted to Dr. R. J. WALLEN of the 'Laboratoire de l'Aimant Permanent' at Orsay (France) for kindly preparing the polonium-source 'made to measure'.

We wish to thank W. ZYCH and F. ZAMBONI who lent us their help in building up the apparatus and their assistance during part of the measurements. We kindly acknowledge the indefatigable aid and competent advice during design and construction of the spectrometer, given to us by Mr. H. SUTER, foreman of the workshop.

This work has been supported by the 'Kommission für Atomwissenschaft' (KAW) of the 'Schweiz. Nationalfonds zur Förderung der wissenschaftlichen Forschung'.

### References

- 1) F. EVERLING, L. A. KÖNIG, J. H. E. MATTAUCH, and A. H. WAPSTRA, Nucl. Phys. **18**, 529 (1960).
- 2) W. G. STURM and V. JOHNSON, Phys. Rev. **83**, 542 (1951).
- 3) C. P. BROWNE, J. A. GALEY, J. R. ERSKINE, and K. L. WARSH, Phys. Rev. **120**, 905 (1960).
- 4) F. BUMILLER, H. H. STAUB, and H. E. WEAVER, Helv. Phys. Acta **29**, 83 (1956).
- 5) A. RYTZ, H. H. STAUB, H. WINKLER, and W. ZYCH, to be published in Helv. Phys. Acta.
- 6) A. RYTZ, H. WINKLER, F. ZAMBONI, and W. ZYCH, Helv. Phys. Acta **34** (1961) (to be published).
- 7) A. RYTZ, Helv. Phys. Acta **34**, 240 (1961).
- 8) H. WINKLER and W. ZYCH, Helv. Phys. Acta **34**, 449 (1961).
- 9) D. R. HARTREE, Proc. Camb. Phil. Soc. **21**, 746 (1923).
- 10) G. BASTIN-SCOFFIER and R. J. WALLEN, Journ. de Phys. et Le Radium **19**, 527 (1958).
- 11) R. L. MACKLIN and J. H. GIBBONS, Phys. Rev. **109**, 105 (1958).
- 12) H. H. STAUB and H. WINKLER, Nucl. Phys. **17**, 271 (1960).

- <sup>13)</sup> R. O. BONDELID, J. W. BUTLER, C. A. KENNEDY, and A. DEL CALLAR, *Phys. Rev.* **120**, 887 (1960).
- <sup>14)</sup> E. R. COLLINS, C. D. MCKENZIE, and C. A. RAMM, *Proc. Roy. Soc. London*, **A 216**, 219 (1953).
- <sup>15)</sup> F. A. WHITE, F. M. ROURKE, J. C. SHEFFIELD, R. P. SCHUMAN, and J. R. HUIZENGA, *Phys. Rev.* **109**, 437 (1958).
- <sup>16)</sup> G. BASTIN-SCOFFIER, Thesis, Fac. des Sciences Paris (1961).
- <sup>17)</sup> R. O. BONDELID and C. A. KENNEDY, *Phys. Rev.* **115**, 1601 (1959).
- <sup>18)</sup> W. E. SHOUPP, B. JENNINGS, and W. JONES, *Phys. Rev.* **76**, 502 (1949).
- <sup>19)</sup> F. EVERLING, L. A. KÖNIG, J. H. E. MATTAUCH, and A. H. WAPSTRA, *Nucl. Phys.* **15**, 342 (1960).
- <sup>20)</sup> A. H. WAPSTRA, *Nucl. Phys.* **18**, 587 (1960).
- <sup>21)</sup> E. H. BECKNER, R. L. BRAMBLETT, G. C. PHILLIPS, and T. A. EASTWOOD, *Phys. Rev.* **123**, 2100 (1961).
- <sup>22)</sup> J. B. MARION, *Rev. Mod. Ph.* **33**, 139 (1961).
- <sup>23)</sup> R. L. DRISCOLL and P. L. BENDER, *Phys. Rev. L.* **1**, 413 (1958).